Vikash Kumar*, Abha Rani and Ajay Kumar Singh

Numerical Solution of Conjugate Free Convection From a Vertical Fin Embedded in a Non-Darcy Porous Medium

https://doi.org/10.1515/zna-2017-0266
Received July 29, 2017; accepted October 29, 2017; previously published online November 30, 2017

Abstract: The problem of conjugate free convection from a vertical fin embedded in a fluid-saturated porous medium is investigated. The governing nonlinear equations are solved iteratively by a highly implicit finite difference scheme. In this paper, the results based on four models, viz the Darcy model, the Brinkman model, the non-Darcian model with nonlinear inertia and viscous terms, and also the non-Darcian model with viscous, nonlinear inertia and velocity square terms, are compared. It is seen that fin cooling is more effective at higher Grashof or Darcy numbers due to stronger convection effects. The local Nusselt number is observed to increase with the Grashof or Darcy numbers and decrease slightly with the conduction–convection parameter. The limitation of the Darcy's law is observed at higher values of permeability when the non-Darcian models are more relevant.

Keywords: Conjugate Free Convection; Highly Implicit Finite Difference Scheme; Non-Darcian Model; Rectangular Fin.

1 Introduction

The problem of conjugate heat transfer from a downward projecting fin immersed in a fluid-saturated porous medium has many important applications such as extraction of geothermal energy and design of insulating system for energy conservation. In conventional heat transfer analysis of fins, it is generally assumed that the convective heat transfer coefficient at the fin surface is uniform all along the fin. The fin heat conduction equation is then solved analytically using a uniform value of the heat transfer coefficient. However, the local fin heat transfer coefficient can experience a substantial variation along the fin surface due to non-uniformities in both the velocity and the temperature fields in the fluid. It is necessary, therefore, to solve the conductive–convective heat transfer as a coupled problem and thereby simultaneously solve for the temperature distributions in the fluid and the fin.

The study of conjugate heat transfer for free convective flow was initiated by Lock and Gunn [1], who have studied boundary layer flow and heat transfer along a thin vertical fin. Bejan and Anderson [2] have examined heat transfer across a vertical partition in a porous medium. They presented an analytical solution for the boundary layer flow and the temperature field around the partition. The conjugate heat transfer from a fin embedded in a porous medium has been investigated by Pop et al. [3] with a high Rayleigh number around a vertical fin. In another paper, Pop et al. [4] analysed the mixed convection heat transfer along a vertical fin using similarity variables to transform the boundary layer equations and solved the resulting equation by using the finite difference method. The problem of conjugate free convection due to a vertical plate in a porous medium is studied by Vynnycky and Shigeo [5] and Kimura et al. [6]. A transient problem of the same nature is studied by Cheng and Pop [7] and Vynnycky and Kimura [8]. Petroudi et al. [9] applied a semi-analytical method for solving a nonlinear equation arising from natural convection around a porous fin by homotopy perturbation method to obtain an approximate solution. Sobamowo et al. [10] considered the thermal performance analysis of a natural convection porous fin with temperature-dependent thermal conductivity and internal heat generation. Conjugate mixed convection heat transfer analysis of a plate fin embedded in a porous medium was performed by Liu et al. [11]. Chen and Chiou [12] have analysed conjugate free convection heat transfer from a vertical fin embedded in non-Darcian porous media. It is worth noting that all the above investigations treat the porous medium as purely Darcian, and boundary

***Corresponding author: Vikash Kumar,** Department of Applied Mathematics, Indian Institute of Technology (Indian School of Mines) Dhanbad, Dhanbad 826004, India,
E-mail: vikashiitism@gmail.com.
http://orcid.org/0000-0002-3669-5807
Abha Rani: Department of Applied Mathematics, Indian Institute of Technology (Indian School of Mines) Dhanbad, Dhanbad 826004, India, E-mail: abharaniiitism@gmail.com
Ajay Kumar Singh: CSIR-Central Institute of Mining and Fuel Research, Dhanbad 826015, India, E-mail: ajay.cimfr@gmail.com

and inertia effects have been totally neglected except in Chen and Chiou [12].

The purpose of the present work was to study the conjugate heat transfer problem along a fin embedded in a fluid-saturated non-Darcian porous medium. The results are based on the inclusion of boundary and inertia effects as well as a nonlinear effect that is invoked to describe the flow. The effects of inertia and viscous forces are taken into account in the momentum equation. These forces are not accounted for in Darcy's law that has been used as the momentum equation by the other researchers. Four models, namely, Darcy model, Brinkman model, non-Darcian model with nonlinear inertia and viscous terms, and also non-Darcian model with viscous, nonlinear inertia and velocity square terms, are considered in the present study. The selection of four individual models described above has been made in order to appreciate the inclusion of viscous, nonlinear inertia and velocity square terms in the momentum equation. The results obtained using the four models are compared, and the importance of viscous and inertia forces has been perceived especially in a highly porous medium. The governing equations are solved iteratively within the framework of boundary layer approximations by a highly implicit finite difference scheme described by Hornbeck [13]. A variable mesh size was used in order to obtain accurate flow and heat transfer characteristics inside the boundary layer.

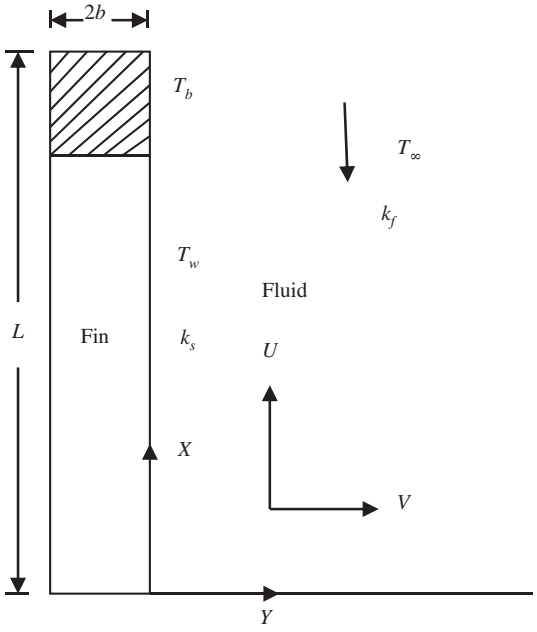

Figure 1: Geometry of the problem.

2 Mathematical Formulations

A slender rectangular fin of thickness $2b$ and length L, as shown in Figure 1, is considered. The fin is placed vertically in a fluid-saturated porous medium, and the base temperature T_b of the fin is taken as prescribed. Heat conduction along the fin is one-dimensional since $2b \ll L$. The fin with a variable wall temperature T_w is in contact with the fluid-saturated porous medium. The temperature T_∞ in the porous medium far away from the fin is considered to be constant. A laminar boundary layer flow is assumed to exist around the fin, and the temperature changes from $T = T_w$ to $T = T_\infty$ within the boundary layer. The direction of the vertical fin is considered as the X direction, and the Y direction is perpendicular to the fin.

The boundary layer is considered to be very thin compared to the length of the fin, and certain approximations in the equations of motion are possible. The fluid is incompressible, and the density is assumed to be constant except in the buoyancy force term according to the Boussinesq approximation. The momentum equation is described by the generalised Darcy's law as proposed by Yamamoto and Iwamura [14] and also by Vafai and Tien [15]. Considering the order of magnitude of the various terms and neglecting the term of equal order of smallness [16] under the framework of boundary layer approximation, the governing equations for the fluid and the fin are given by

$$\frac{\partial U}{\partial X} + \frac{\partial V}{\partial Y} = 0 \tag{1}$$

$$U\frac{\partial U}{\partial X} + V\frac{\partial U}{\partial Y} = \mu\frac{\partial^2 U}{\partial Y^2} + g\beta(T - T_\infty) - \frac{\mu U}{K} - \frac{C_F \rho U^2}{\sqrt{K}} \tag{2}$$

$$U\frac{\partial T}{\partial X} + V\frac{\partial T}{\partial Y} = \alpha\frac{\partial^2 T}{\partial Y^2} \tag{3}$$

$$\frac{\mathrm{d}^2 T_w}{\mathrm{d}X^2} + \frac{k_f}{k_s b}\left[\frac{\partial T}{\partial Y}\right]_w = 0 \tag{4}$$

While the last term, that is, the velocity square term in (2) is considered in the non-Darcian model considered by Vafai and Tien [15], the term vanishes in the model proposed by Yamamoto and Iwamura [14].

The boundary conditions are,

$$\begin{aligned} &Y = 0:\ U = 0,\ V = 0,\ T = T_w(X) \\ &Y \to \infty:\ U \to 0,\ T \to T_\infty \\ &X = 0:\ U = 0,\ T = T_\infty,\ \frac{\mathrm{d}T_w}{\mathrm{d}X} = 0 \\ &X = L:\ T_w = T_b \end{aligned} \tag{5}$$

where U and V are the vertical and horizontal velocity components, T is the fluid temperature, and T_∞, T_w and T_b are the temperatures of the ambient fluid, fin surface, and fin base, respectively. Also, g is the acceleration due to gravity, β is the coefficient of volume expansion, μ is the kinematic viscosity, C_F is the inertia coefficient, α is the thermal diffusivity, k_f and k_s are the thermal conductivities of the fluid and the fin, and K is the permeability of the porous medium.

Since the fluid is in contact with the fin at $Y=0$, the velocity components are taken as zero because of the no-slip condition and the fluid temperature is equal to the temperature of the fin surface. With the temperature boundary condition for the fluid at $Y=0$, the wall temperature T_w is unknown and needs to be solved through the heat conduction equation for the fin. The vertical velocity component U and the fluid temperature outside the boundary layer ($Y\to\infty$) are equal to the free stream velocity and temperature, respectively. The boundary condition for the horizontal velocity component V at $Y\to\infty$ is not required, as the second-order derivative of V with respect to Y does not occur anywhere in the equation. The vertical velocity component U and the fluid temperature at bottom of the fin ($X=0$) are equal to the free stream velocity and temperature, respectively. The fin base temperature T_b at $X=L$ is prescribed.

Introducing the following dimensionless quantities,

$$u=\frac{UL}{\mu},\ v=\frac{VL}{\mu},\ \theta=\frac{T-T_\infty}{T_b-T_\infty},\ \theta_w=\frac{T_w-T_\infty}{T_b-T_\infty},$$
$$x=\frac{X}{L},\ y=\frac{Y}{L},\ \mathrm{Da}=\frac{K}{L^2},$$
$$\mathrm{Gr}=\frac{g\beta(T_b-T_\infty)L^3}{\mu^2},\ \mathrm{CCP}=\frac{k_fL}{k_sb},\ \mathrm{Pr}=\frac{\mu}{\alpha} \tag{6}$$

the governing (1)–(4) take the following dimensionless form:

$$\frac{\partial u}{\partial x}+\frac{\partial v}{\partial y}=0 \tag{7}$$

$$u\frac{\partial u}{\partial x}+v\frac{\partial u}{\partial y}=\frac{\partial^2 u}{\partial y^2}+\mathrm{Gr}\theta-\frac{u}{\mathrm{Da}}-\frac{u^2C_F}{\sqrt{\mathrm{Da}}} \tag{8}$$

$$u\frac{\partial \theta}{\partial x}+v\frac{\partial \theta}{\partial y}=\frac{1}{\mathrm{Pr}}\frac{\partial^2\theta}{\partial y^2} \tag{9}$$

$$\frac{\mathrm{d}^2\theta_w}{\mathrm{d}x^2}+\mathrm{CCP}\left[\frac{\partial\theta}{\partial y}\right]_w=0 \tag{10}$$

where Gr is the Grashof number, Pr is the Prandtl number, C_F is the inertia coefficient, Da is the Darcy number, and CCP is the conduction–convection parameter.

Equations (7)–(10) are to be solved with the following dimension boundary conditions:

$$\begin{aligned} &y=0:\ u=0,\ v=0,\ \theta=\theta_w(x)\\ &y\to\infty:\ u\to0,\ \theta\to0\\ &x=0:\ u=0,\ \theta=0,\ \frac{\mathrm{d}\theta_w}{\mathrm{d}x}=0\\ &x=1:\ \theta_w=1 \end{aligned} \tag{11}$$

The boundary condition for θ_w at $x=0$ is based on the following argument. If the fin is very long and thin, the amount of heat that passes from the tip of the fin to the fluid is negligible as compared to the heat loss through the lateral surface. In such a case, the assumption of an adiabatic tip is justified and the temperature gradient in the fin at the tip is thus assumed to be zero.

It may also be observed that in the foregoing description of the boundary conditions, no mention is made of the velocity at the base surface. This omission is required by the boundary layer equations. Once the conditions have been specified at the leading edge of the plate ($x=0$), the solution yields the velocity field at all small values of $x>0$ and, therefore, does not permit specification of the velocity boundary condition at any value of $x>0$. The non-accounting of the hydrodynamic effects related to the presence of the base surface should not materially affect the fin heat transfer results provided the fin length L is large compared with the boundary layer thickness at $x=L$ [17].

3 Method of Solution

The finite difference form of (7)–(10) was solved numerically by superposing a two-dimensional rectangular mesh on the flow field. A highly implicit numerical scheme [13] was used for the difference representation of the momentum and energy equations in which not only all y derivatives were evaluated at the unknown level but also the coefficient of nonlinear convective terms was taken at the unknown level. This form is necessitated by the zero velocity of the free stream, which will result in the classical implicit formulation being inconsistent. The continuity equation has been written in explicit form. Since the difference form is nonlinear, an iterative scheme was applied to solve the system of difference equations one by one in a sequential manner. The process involves an overall iteration loop between the fluid and the fin equation and a sub-iteration loop for the fluid-phase equations. The basic steps of the procedure are summarised below:

(a) An initial guess for the fin temperature $\theta_w(x)$ is estimated. A parabolic variation, say $\theta_w(x)=x^2$, was found to be a good initial guess.
(b) The flow field and convective heat transfer equations in the fluid are solved with the guessed fin temperature distribution as the wall boundary condition.

(c) From the calculated fluid temperature field, the heat flux $\left(\frac{\partial\theta}{\partial y}\right)_w$ is estimated at every x position.

(d) The fin heat conduction equation is solved by prescribing the value of $\left(\frac{\partial\theta}{\partial y}\right)_w$ as obtained above, which gives a new distribution of the fin temperature.

(e) With a new guess for the temperature distribution evaluated from their current values, steps (b)–(d) are repeated until convergence is obtained. Finally, all the relevant heat transfer characteristics are calculated.

It may not be out of place to mention that the highly implicit numerical scheme was used to solve the set of nonlinear steady-state (8) and (9) as it was found to be consistent. Hornbeck [13] has used such a method to solve similar mathematical equations.

The computer program takes care of the fact that the velocity and temperature profiles vary rapidly near the fin, and hence, a fine mesh is required near the fin. A relatively coarse mesh has been used in the regions of slower variation.

4 Results and Discussion

To establish the correctness of the present work, the results obtained by the finite difference method are compared with analytical solutions for a limiting case corresponding to a free fluid (Da→∞) flow at a low Grashof number. In this case, the energy equation reduces to

$$\frac{d^2\theta}{dy^2}=0 \tag{12}$$

The general solution of the above equation, which satisfies the given boundary condition, is

$$\theta=\theta_w(x)\left(1-\frac{y}{y_{max}}\right) \tag{13}$$

where $\theta_w(x)=\frac{\cosh(mx)}{\cosh(m)}$ and $m^2=\frac{CCP}{y_{max}}$ for CCP≠0. For CCP = 0, there is no heat loss from the fin and the entire fin is assumed to be at constant temperature equal to the base temperature. So, one can set $\theta_w(x)=1$ for CCP = 0.

Neglecting the inertial and Darcy resistance terms, the equation of motion can be written in a simplified form as,

$$\frac{d^2u}{dy^2}+Gr\theta=0 \tag{14}$$

The solution of (14) with the given velocity boundary condition is,

$$u=Gr\left(\frac{y^3}{6y_{max}}-\frac{y^2}{2}-\frac{yy_{max}}{3}\right) \tag{15}$$

The results corresponding to the above-described limiting case, obtained by the finite difference method, are compared with the exact analytical values in Table 1.

The good agreement between the numerical and exact analytical solutions indicates the correctness of the results obtained by the finite difference method.

After validation of the numerical scheme followed in the present study, numerical results have been obtained by using the following four models:

I. Darcy's model
II. Brinkman model
III. Non-Darcian model with nonlinear inertia and viscous terms
IV. Non Darcian model with viscous, nonlinear inertia and velocity square terms.

The wall temperature variation with x is plotted for various values of Gr in Figure 2. The analytical result obtained for small values of Gr is shown by a broken line. It is found that as Gr decreases, the temperature profile approaches

Table 1: Temperature and velocity distribution for Da→∞(10^3), CCP = 0, Gr = 1.0 and y_{max} = 0.81.

y	Temperature		Horizontal velocity	
	Numerical results	Analytical results	Numerical results	Analytical results
0.0	1.0000	1.0000	0.0000	0.0000
0.1	0.8780	0.8765	0.0225	0.0222
0.2	0.7560	0.7531	0.0363	0.0356
0.3	0.6340	0.6296	0.0425	0.0416
0.4	0.5120	0.5062	0.0423	0.0412
0.5	0.3901	0.3827	0.0371	0.0357
0.6	0.2681	0.2593	0.0279	0.0264
0.7	0.1462	0.1358	0.0160	0.0146

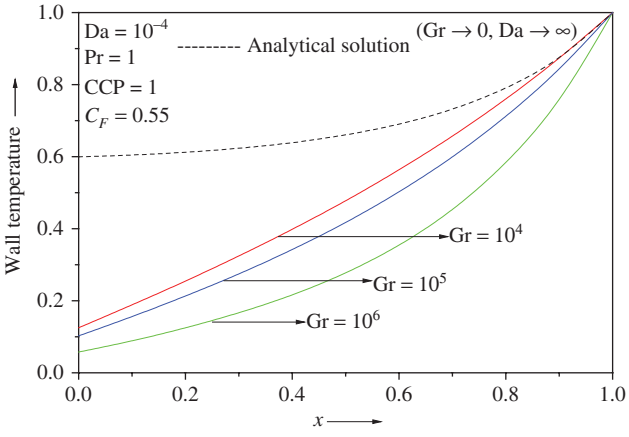

Figure 2: Effect of Gr on wall temperature.

the hyperbolic variation as suggested by the analytical solution (CCP ≠ 0 and low Gr). As Gr increases, more heat is removed from the fin by fluid convection as indicated by the slope of the wall temperature.

The wall temperature variation for various values of the Darcy number is shown in Figure 3. It is seen that as the Darcy number approaches zero, the wall temperature distribution moves closer to the analytical solution for pure conduction in the fluid. This is to be expected since for small values of Da, the Darcy resistance to flow is very large, reducing the velocity of the fluid. The heat convection effect, therefore, becomes very small even at large values of Gr as Da approaches zero. Thus, for increasing Da, the fin is cooled more.

In Figure 4, the effect of the conduction–convection parameter CCP upon the wall temperature distribution is depicted. For each value of CCP, the numerical solution and the corresponding pure conduction solution have been plotted. The trend is acceptable since higher CCP leads to more coupling between the solid and the fluid phases and, hence, more heat loss from the fin. Both the analytical and numerical solutions exhibit a similar variation with CCP, although a close match between the numerical and its corresponding analytical solution is not to be expected on account of the high Gr value used for the numerical solutions.

In Figure 5, the fluid temperature variation in the x direction is shown for various values of the Grashof number at a fixed value of y. As the Grashof number increases, the temperature of the fluid decreases. This trend is similar to that of the fin temperature. Although the total amount of heat removed from the fin is larger at a higher Grashof number, the increase in the heat transfer coefficient is more rapid, resulting in a smaller fluid temperature.

Figures 6 and 7 show the variation of the temperature and the velocity fields in the y direction at various x locations. As expected, for fixed values of the other parameters, the velocity and temperature values increase with x. The increase in the velocity values with x indicates that

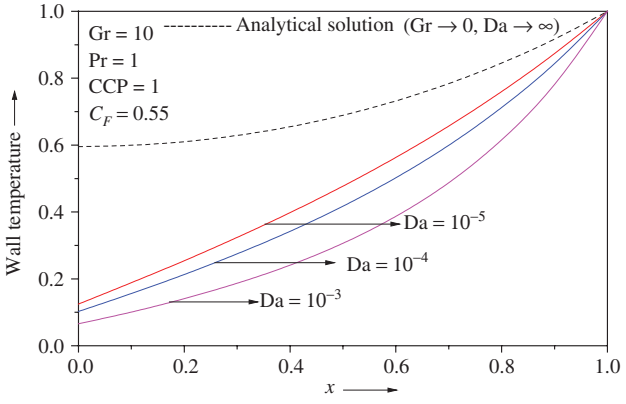

Figure 3: Effect of Da on wall temperature.

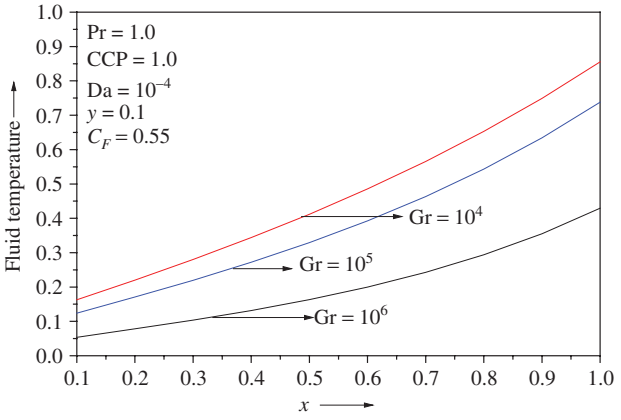

Figure 5: Fluid temperature profile.

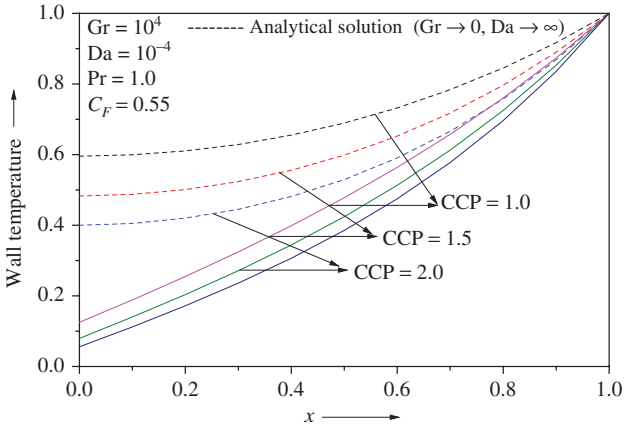

Figure 4: Effect of CCP on wall temperature.

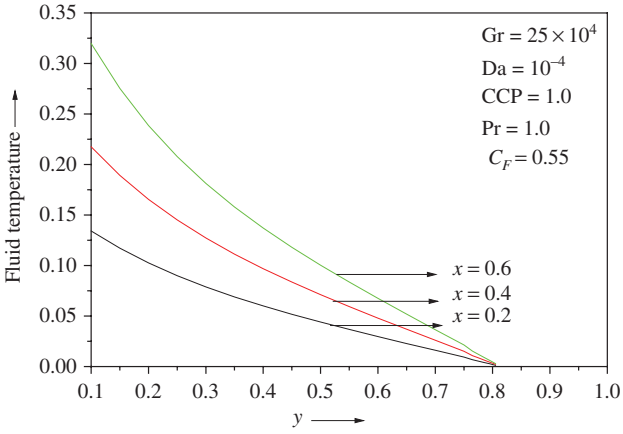

Figure 6: Fluid temperature distribution.

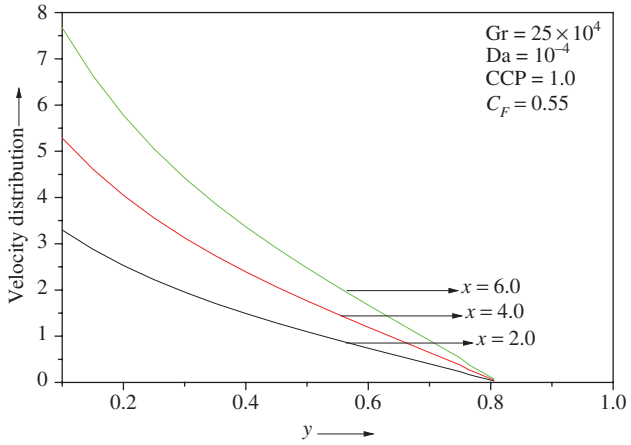

Figure 7: Vertical velocity distribution.

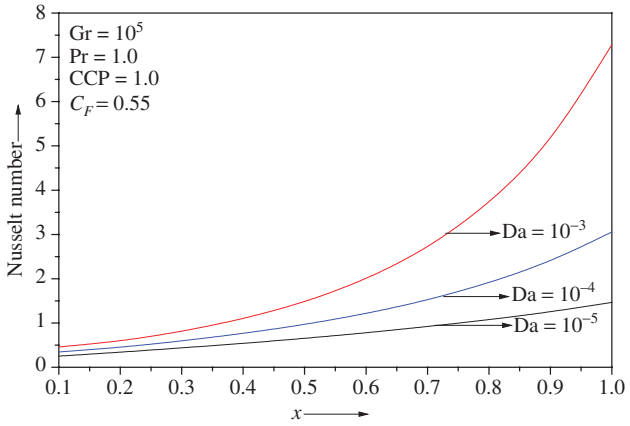

Figure 9: Effect of Da on the Nusselt number.

natural convection becomes more and more vigorous as fluid flow advances to the fin base in the x direction. This is a direct consequence of increased heat penetration into the fluid at higher values of x.

In Figures 8–10, the local Nusselt number variation with the governing parameters Gr, Da, and CCP are shown. The Nusselt number increases with Gr and Da and it decreases slightly with CCP. Since the heat loss from the fin is related to the slope of the wall temperature variation in the x direction and the Nusslet number characterises heat loss from the fin, the observed variation of the Nusslet number with various parameters can be explained by considering the slope of θ_w in Figures 2–4.

In Figure 11, the wall temperature profile predicted by the present analysis is compared with that of Pop et al. [4], who have considered Darcy's model for flow. The result of Pop et al. [4] is shown by a broken line. For a smaller Grashof number, the difference is not significant. However, as expected, the non-Darcy effects play an important role at higher Grashof numbers.

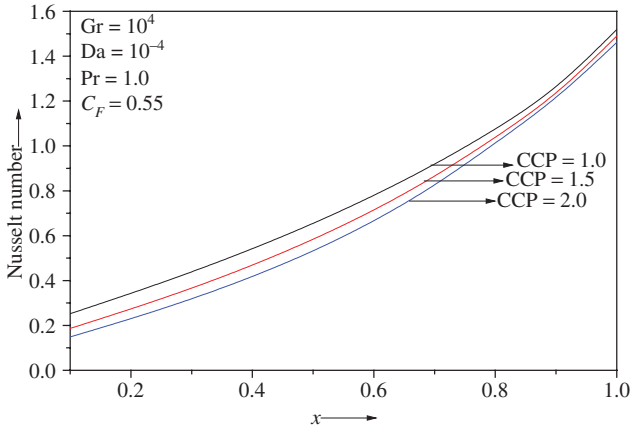

Figure 10: Effect of CCP on the Nusselt number.

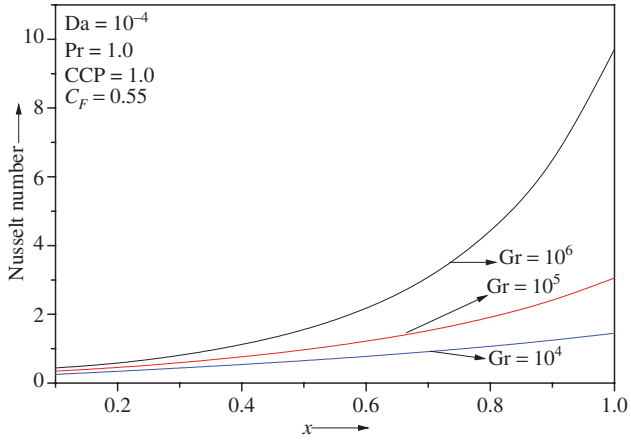

Figure 8: Effect of Gr on the Nusselt number.

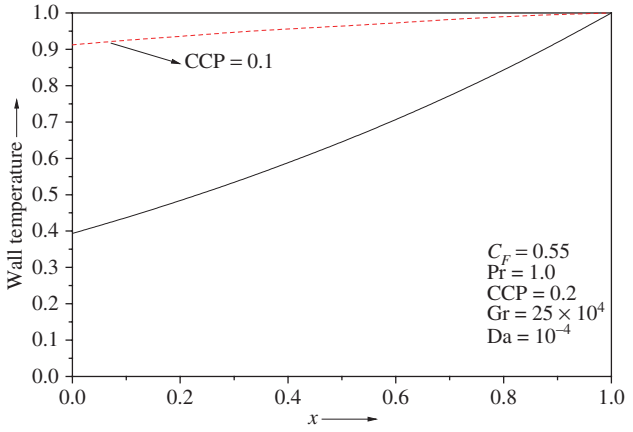

Figure 11: Comparison with the Darcian regime.

In Figure 12a–c, the wall temperature has been shown as a function of x. Results based on the four models I, II, III, and IV are presented below.

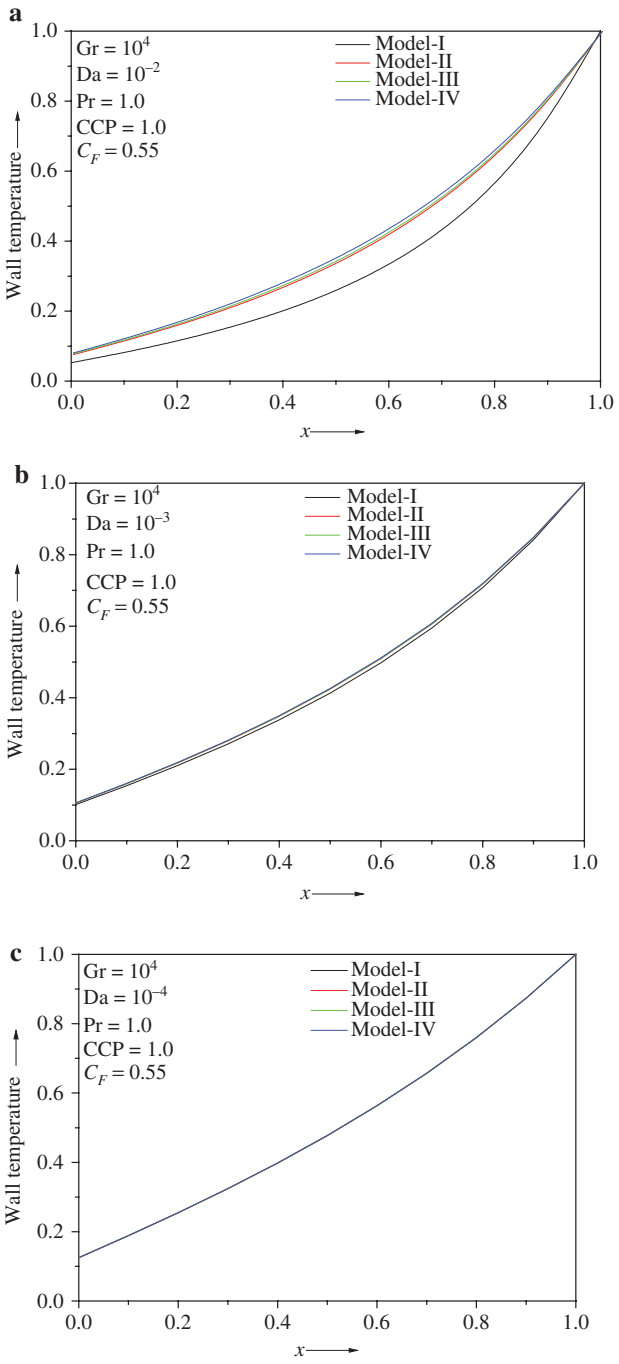

Figure 12: (a) Wall temperature comparison using four different models for Da = 10^{-2}. (b) Wall temperature comparison using four different models for Da = 10^{-3}. (c) Wall temperature comparison using four different models for Da = 10^{-4}.

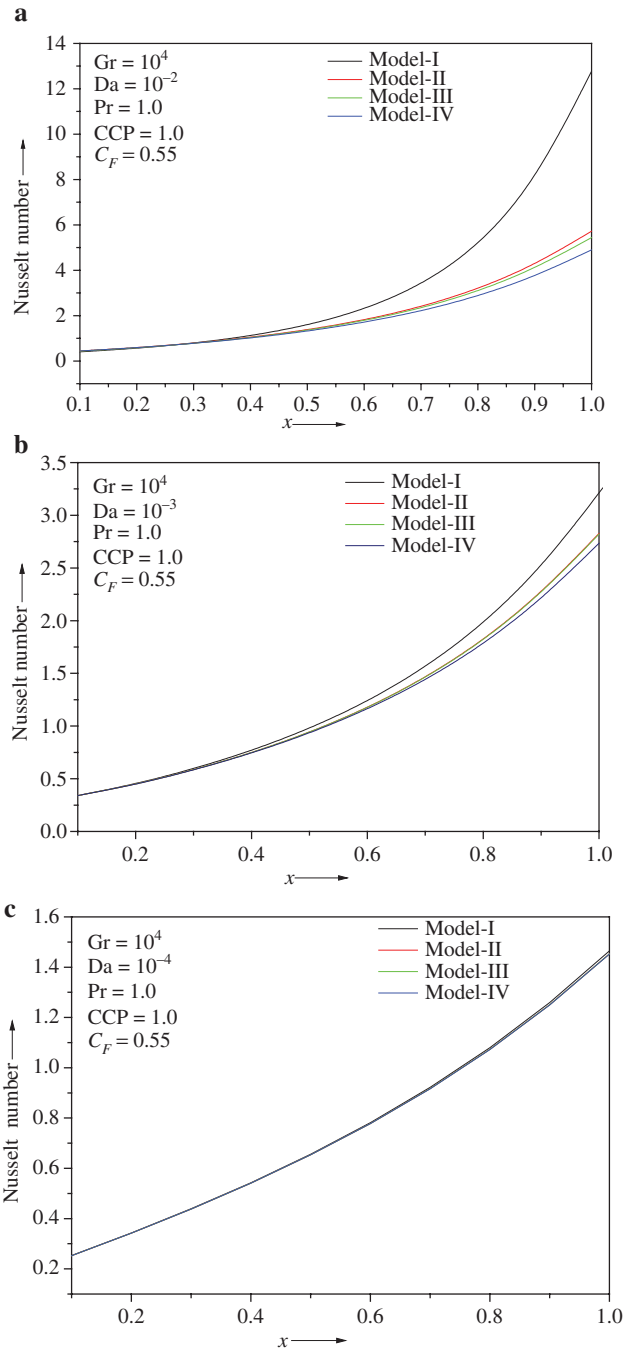

Figure 13: (a) Comparison of local Nusselt number using four different models for Da = 10^{-2}. (b) Comparison of local Nusselt number using four different models for Da = 10^{-3}. (c) Comparison of local Nusselt number using four different models for Da = 10^{-3}.

It is seen that the wall temperature values obtained by using all the four models are very close at Da = 10^{-4}, and variation in results is observed at higher values of the Darcy number (Da). A similar trend is observed in the local Nusselt number also with increasing values of the Darcy number as depicted in Figure 13a–c.

This trend is attributed to the limitations of the Darcy's model at higher value of permeability when inertia forces cannot be neglected. It is imperative, therefore, to apply non-Darcian models at greater permeability like the highly fractured reservoirs.

5 Conclusion

The conductive–convective heat transfer from a fin embedded in a porous medium has been modelled as a coupled problem, and the temperature distributions in the fluid and the fin have been solved simultaneously. Inertia and viscous forces are accounted for by using generalised non-Darcian models to obtain better results, particularly in the case of a highly permeable porous medium adjacent to an impermeable surface. The problem is governed by some dimensionless parameters, viz the Grashof number, the Darcy number, the conduction–convection parameter, and the inertia coefficient. Numerical solutions of the problem are obtained by a highly implicit finite difference method. A non-uniform grid is adopted in order to obtain accurate flow and heat transfer characteristics inside the boundary layer. The fin cooling is observed to be more effective at a higher Grashof or Darcy number due to stronger convection effects. It is observed that the local Nusselt number increases with the Grashof and Darcy numbers and decreases slightly with the conduction–convection parameter as more heat is removed from the fin at higher Grashof and Darcy numbers, but higher CCP leads to greater coupling between the solid and fluid phases. It has been found that the application of the non-Darcian models is essential in the case of a highly porous medium.

Acknowledgments: The authors gratefully acknowledge the valuable suggestions of Professor T. Sundararajan, Department of Mechanical Engineering, Institute of Technology Madras, Chenai, India.

References

[1] G. S. Lock and J. C. Gunn, J. Heat Transfer **90**, 63 (1968).
[2] A. Bejan and R. Anderson, Int. J. Heat Mass Transfer **24**, 1237 (1981).
[3] I. Pop, J. K. Sunada, P. Cheng, and W. J. Minkowycz, Int. J. Heat Mass Transfer **28**, 1629 (1985).
[4] I. Pop, D. B. Ingham, P. J. Heggs, and D. Gardner, In Proc. 8th Int. Heat Transfer Conference, San Francisco, CA, 2635 (1986).
[5] M. Vynnycky and K. Shigeo, Int. J. Heat Mass Transfer **37**, 229 (1994).
[6] S. Kimura, A. Okajima, and T. Kiwata, Int. J. Heat Mass Transfer **41**, 3203 (1998).
[7] P. Cheng and I. Pop, Int. J. Eng. Sci. **22**, 253 (1984).
[8] M. Vynnycky and S. Kimura, Int. J. Heat Mass Transfer **38**, 219 (1995).
[9] R. I. Petroudi, D. D. Ganji, B. A. Shotorban, K. M. Nejad, E. Rahimi, et al., Thermal Sci. **16**, 1303 (2012).
[10] M. G. Sobamowo, O. M. Kamiyo, and O. A. Adeleye, Thermal Sci. Eng. Prog. **1**, 39 (2017).
[11] J. Y. Liu, W. J. Minkowycz, and P. Cheng, Numer. Heat Transfer A Appl. **9**, 575 (1986).
[12] C. H. Chen and J. S. Chiou, Int. J. Eng. Sci. **32**, 1703 (1994).
[13] R. W. Hornbeck, Numerical Marching Techniques for Fluid Flows with Heat Transfer, NASA, Washington, DC 1973.
[14] K. Yamamoto and N. Iwamura, J. Eng. Math. **10**, 41 (1976).
[15] K. Vafai and C. L. Tien, Int. J. Heat Mass Transfer **24**, 195 (1981).
[16] A. Bejan, Convection Heat Transfer, John Wiley & Sons, New York 2013.
[17] B. Sundén, Int. Commun. Heat Mass Transfer **10**, 267 (1983).